

Recent Results from RENO

Hyunkwan Seo¹ for the RENO Collaboration

Seoul National University

1 Gwanak-ro, Gwanak-gu, Seoul 151-742, Korea

E-mail: hkseo16@gmail.com

The Reactor Experiment for Neutrino Oscillation (RENO) started data-taking from August, 2011 and has measured the smallest neutrino mixing angle θ_{13} by observing the disappearance of reactor antineutrinos. RENO has accumulated roughly 800 days of data, which enable to make an accurate measurement of the reactor neutrino flux and spectral shape. Antineutrinos from the six reactors at Hanbit Nuclear Power Plant in Korea are detected and compared by the two identical detectors located in the near and far distances from the reactor array center. We present new results on precisely measured $\sin^2 2\theta_{13}$ value as well as reactor neutrino flux and spectrum based on the 800 days of data sample.

*16th International Workshop on Neutrino Factories and Future Neutrino Beam Facilities
25 -30 August, 2014
University of Glasgow, United Kingdom*

¹Speaker

1. Introduction

Since RENO published the result of the measurement of the smallest neutrino mixing angle θ_{13} in [1], RENO has been updating its result using increased statistics and improved systematics. In addition, we have started the analysis of the neutron capture on Hydrogen and spectral shape analysis. The experiment has accumulated roughly 800 live days of data until Dec. 2013 and its data-taking is still continuing. We report the improved results of θ_{13} measurement using the 800 live days of data.

2. Experimental setup and detectors

RENO detects antineutrinos from the six reactors at Hanbit Nuclear Power plant in Yonggwang, Korea. The arrangement of the reactors and the detectors are shown in Figure 1. The six pressurized water reactors with each maximum thermal output of $2.8 \text{ GW}_{\text{th}}$ (reactors 3, 4, 5 and 6) or $2.66 \text{ GW}_{\text{th}}$ (reactors 1 and 2) are lined up in roughly equal distances and span ~ 1.3 km. Two identical antineutrino detectors are located at 294 m and 1383 m, respectively, from the center of reactor array. The far (near) detector is beneath a hill that provides 450 m (120 m) of water equivalent rock overburden to reduce the cosmic backgrounds. The far-to-near ratio of antineutrino fluxes measured in the two identical detectors can considerably reduce systematic errors coming from uncertainties in the reactor neutrino flux, target mass, and detection efficiency. The reactor-flux weighted baseline is 408.56 m for the near detector, and 1443.99 m for the far detector.

Each RENO detector (Figure 2) consists of a main inner detector (ID) and an outer veto detector (OD). The main detector is contained in a cylindrical stainless steel vessel that houses two nested cylindrical acrylic vessels. The innermost acrylic vessel holds 18.6 m^3 (16.5 t) $\sim 0.1\%$ Gadolinium (Gd) doped liquid scintillator (LS) as a neutrino target. An electron antineutrino can interact with a free proton in LS. The coincidence of a prompt positron signal and a delayed signal from neutron capture by Gd provides the distinctive signature of inverse β -decay (IBD).

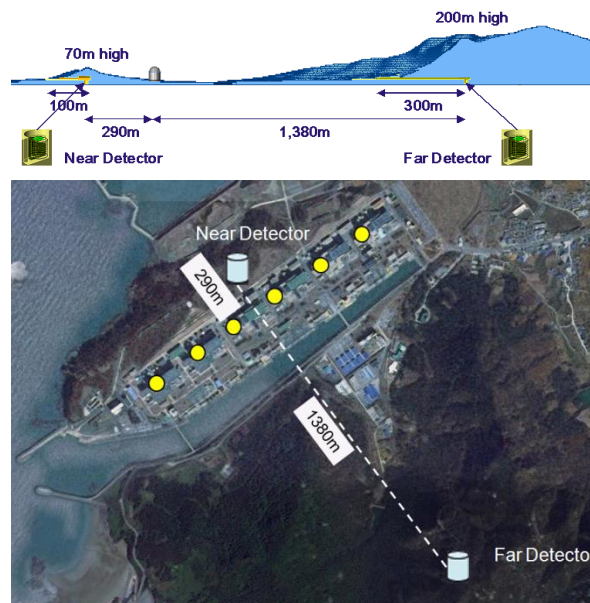


Figure 1. A schematic setup of the RENO experiment.

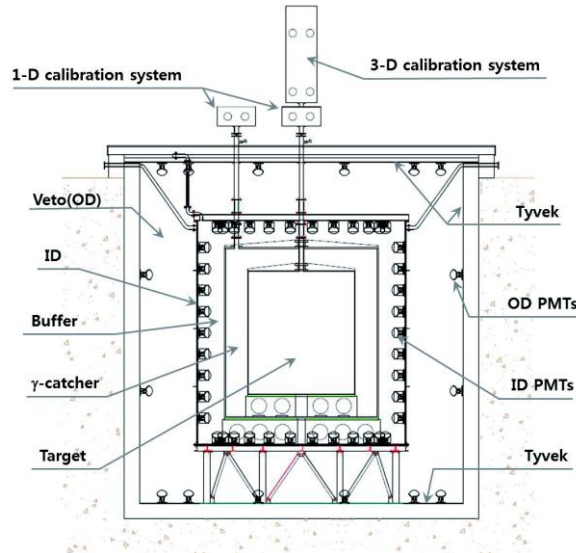


Figure 2. A schematic view of the RENO detector. The near and far detectors are identical.

The central target volume is surrounded by a 60 cm thick layer of LS without Gd, useful for catching γ -rays escaping from the target region and thus increasing the detection efficiency. Outside this γ -catcher, a 70 cm thick buffer-layer of mineral oil provides shielding from radioactivity in the surrounding rocks and in the 354 10-inch Hamamatsu R7081 photomultiplier tubes (PMTs) that are mounted on the inner wall of the stainless steel container, providing 14% surface coverage. The outermost veto layer of OD consists of 1.5 m of highly purified water in order to identify events coming from outside by their Cherenkov radiation and to shield against ambient γ -rays and neutrons from the surrounding rocks. The OD is equipped with 67 10-inch R7081 water-proof PMTs mounted on the wall of the veto vessel. The whole surfaces of OD are covered with Tyvek sheets to increase the light collection. The more detail of detection methods and setup of the RENO experiment can be found elsewhere [2]

3. Data analysis

With the 800 live days of data taken from 11 August 2011 to 31 December 2013, the far (near) detector observed 50,750 (433,196) electron antineutrino candidate events with a background fraction of 7.1 % (2.2 %). In this section, the analysis for the IBD events with neutron captured by Gd is described.

3.1 Event selection

Event triggers are formed by the number of PMTs with signals above ~ 0.3 photoelectron (p.e.) threshold (NHIT). An event is triggered and recorded if the ID NHIT is larger than 90, corresponding to 0.5 \sim 0.6 MeV well below the 1.02 MeV as the minimum energy of an IBD positron signal, or if the OD NHIT is larger than 10. The event energy is measured based on the total charge (Q_{tot}) in p.e., collected by the PMTs. The following criteria are applied to select IBD candidate events: (i) $Q_{max}/Q_{tot} < 0.03$ where Q_{max} is the maximum charge of a PMT, to eliminate PMT flasher events and external γ -ray events; (ii) a cut rejecting events that occur within a 1 ms window following a cosmic muon traversing the ID with an energy deposit (E) that is larger

than 70 MeV, or with E between 20 MeV and 70 MeV for OD NHIT > 50; (iii) events are rejected if they are within a 700 ms window following a cosmic muon traversing the ID if E is larger than 1.5 GeV; (iv) $0.7 \text{ MeV} < E_p < 12.0 \text{ MeV}$; (v) $6.0 \text{ MeV} < E_d < 12.0 \text{ MeV}$, where E_p (E_d) is the energy of prompt (delayed) event; (vi) $2 \mu\text{s} < \Delta t_{e+n} < 100 \mu\text{s}$, where Δt_{e+n} is the time difference between the prompt and delayed signals; (vii) a multiplicity requirement rejecting correlated coincidence pairs if they are accompanied by any preceding ID or OD trigger within a 100 μs window before their prompt candidate.

3.2 Backgrounds

After applying all the selection criteria, uncorrelated and correlated backgrounds still survive. The uncorrelated background is due to accidental coincidences from random association of a prompt-like event due to radioactivity and a delayed-like neutron capture. The remaining rate in the final sample is estimated to be 1.82 ± 0.11 per day for near and 0.36 ± 0.01 per day for far. For the correlated backgrounds, there are three types of background: Fast neutrons, ${}^9\text{Li}/{}^8\text{He}$ and ${}^{252}\text{Cf}$. Fast neutrons are produced by cosmic muons traversing the surrounding rocks or the detector. An energetic neutron entering the ID can interact in the target to produce a recoil proton before being captured on Gd. The estimated fast neutron background is 2.09 ± 0.06 per day for near and 0.44 ± 0.02 per day for far. The ${}^9\text{Li}/{}^8\text{He}$, β -n emitters are mostly produced by energetic muons because their production cross sections in carbon increase with muon visible energy [3][4][5]. The ${}^9\text{Li}/{}^8\text{He}$ background rate in the final sample is obtained as 8.28 ± 0.66 per day for near and 1.85 ± 0.20 per day for far from a fit to the decay time distribution with an observed mean decay time of $\sim 250 \text{ ms}$. ${}^{252}\text{Cf}$ background has appeared since the end of September 2012 due to a leakage of tiny fraction of ${}^{252}\text{Cf}$ source during RENO calibration work. The ${}^{252}\text{Cf}$ background shape is obtained by subtracting all the other three backgrounds from IBD candidates and the rate was estimated by fitting IBD candidates with IBD signal and all background spectral functions. The ${}^{252}\text{Cf}$ background rate in the final sample is estimated to be 0.28 ± 0.05 per day for near and 1.98 ± 0.27 per day for far.

In summary, the total background rates are 12.48 ± 0.68 (near) and 4.62 ± 0.28 (far) events per day.

3.3 Systematic uncertainty

The absolute uncertainties of the detection efficiencies are correlated between the two detectors. The uncertainties of the detection efficiencies are dominated by uncertainties associated with spill-in events of IBD events that occur outside the target and produce a neutron capture on Gd in the target, Gd capture ratio, target protons, delayed energy cut, time coincidence cut and IBD cross section. The combined absolute uncertainty of the detection efficiency is estimated as 1.29 %. Only differences between the two identical detectors are taken as uncorrelated relative uncertainties. They come from relative differences between the detectors in energy scale, target protons, and Gd capture ratio. The combined uncorrelated detection uncertainty is estimated to be 0.2 %.

The reactor antineutrino flux depends on thermal power, fission fractions of the four isotopes, energy released per fission, and fission and capture cross sections. The uncertainties associated with the reactor antineutrino flux are 2.0 % and 0.9 % for correlated and uncorrelated errors, respectively, as described in [1].

4. Result

The value of $\sin^2\theta_{13}$ is determined from a χ^2 fit with pull terms on the uncorrelated systematic uncertainties. The best-fit value obtained using the 800 live days of data is

$$\sin^2\theta_{13} = 0.101 \pm 0.008 \text{ (stat.)} \pm 0.010 \text{ (syst.)},$$

and excludes the no-oscillation hypothesis at the 7.8 standard deviation level.

During the data-taking period, some reactors were off for fuel replacement or unscheduled maintenance. Figure 3 presents the time variation of the measured daily rates of IBD candidates after background subtraction in the near and far detectors. Figure 4 shows the correlation of IBD rate (/day) and expected IBD rate (/day) in the best fit value. The fitted slope is 0.998 ± 0.010 and the fitted interception is 0.207 ± 0.856 , which indicate that our background subtraction is correct. By comparing the observed IBD prompt spectrum with the prediction obtained using reactor neutrino flux models by Mueller [6] and Huber [7], we have observed the excess of events around 5 MeV as shown in Figure 5. The amount of the excess is around 2 % of the measured IBD prompt signal. We also have observed the 5 MeV excess has a clear correlation with reactor thermal power as shown in Figure 6.

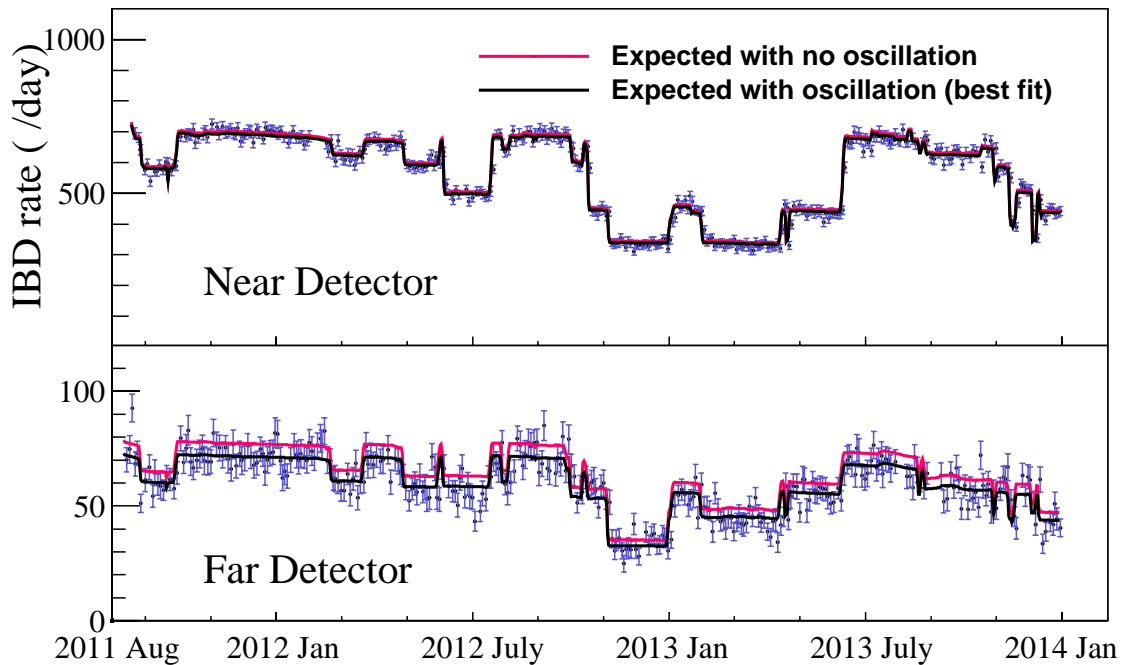


Figure 3. Daily rates of IBD candidates after background subtraction in the near and far detectors. The solid lines are the predicted rates without (in red) and with (in black) oscillation.

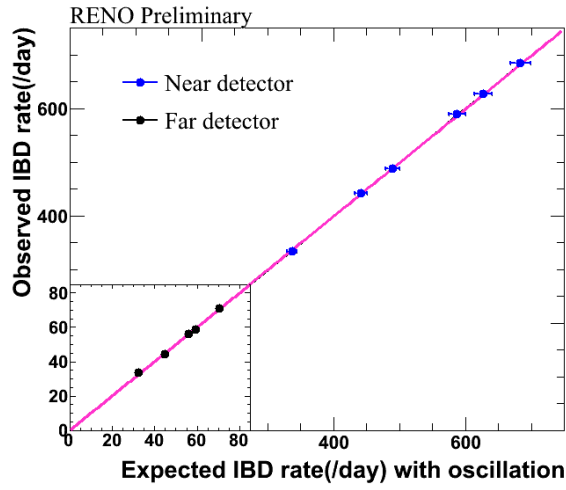


Figure 4. Observed IBD rate (/day) versus expected IBD rate (/day) with oscillation.

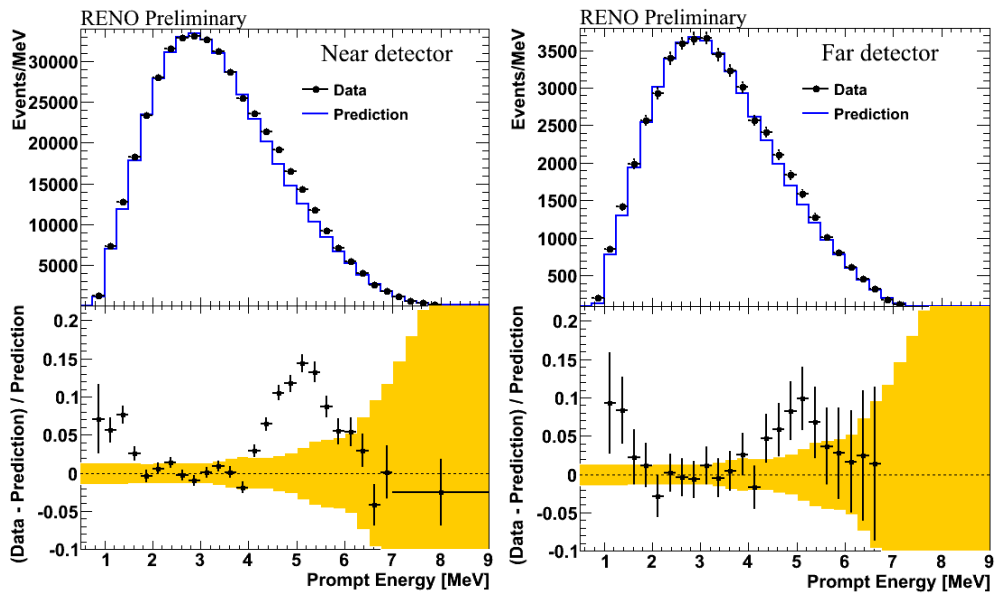


Figure 5. Comparison of the observed IBD prompt spectrum with the prediction with oscillation. The excess of events around 5MeV are observed.

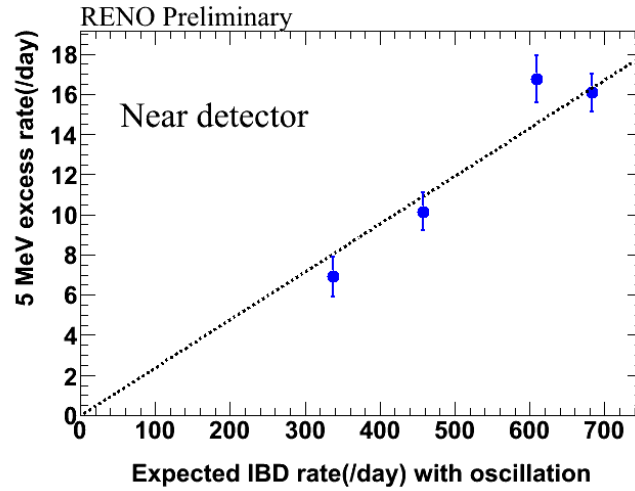


Figure 6. Correlation of the 5 MeV excess and reactor thermal power obtained in near detectors.

5. Summary and Prospect

RENO has improved the measurement of $\sin^2 2\theta_{13}$ with increased data sample and better systematics based on rate-only analysis. The newly measured value is $\sin^2 2\theta_{13} = 0.101 \pm 0.008$ (stat.) ± 0.010 (syst.), corresponding to 7.8σ (13 % precision). Our goal is to reach 7 % precision using 5 years of data. We have observed that excess of IBD events at around 5 MeV compared to the predictions and the excess has a correlation with reactor thermal power. The analysis of energy spectra is on-going using the same data set. In addition, the analysis of the neutron capture on Hydrogen and sterile neutrino search are in progress.

References

- [1] J.K.Ahn *et al.* (RENO Collaboration), *Observation of Reactor Electron Antineutrinos Disappearance in the RENO Experiment*, Phys.Rev.Lett. **108**, 191802 (2012).
- [2] J.K.Ahn *et al.* (RENO Collaboration), arXiv:1003.1391.
- [3] T. Hagner *et al.* Astropart. Phys. **14**, 33 (2000).
- [4] D.R. Tilley, J.H. Kelleys, J.L. Godwin, D.J. Millener, J.E. Purcell, C.G. Sheu, H.R. Weller, Nucl. Phys. **A745**, 155 (2004).
- [5] S. Abe *et al.* (KamLAND Collaboration), Phys. Rev. C **81**, 025807 (2010).
- [6] Th. A. Mueller *et al.*, Phys. Rev. C **83** 054615 (2011).
- [7] P. Huber, Phys. Rev. C **84**, 024617 (2011).